Area fraction quantification of ferroelectric domain orientations in $BaTiO_3$ using piezoresponse force microscopy

Rodrigo P. Fernandes,[1] Ralf-Peter Herber,[2] Lothar Kunz,[3] Henry E. Mgbemere,[1] and Gerold A. Schneider[1,a)]
[1]*Institute of Advanced Ceramic, Hamburg University of Technology, Hamburg 21073, Germany*
[2]*Department of Orofacial Sciences, University of California, San Francisco, 707 Parnassus Avenue, D-2256, P. O. Box 0438, San Francisco, California 94143, USA*
[3]*Robert Bosch GmbH, Postfach 10 60 50, 70049 Stuttgart, Germany*

(Received 25 March 2010; accepted 27 June 2010; published online 19 August 2010)

Understanding the domain structure of ferroelectric ceramics is very important to develop sound knowledge of the influence of the microstructure on the macroscopic properties. To proceed in this direction, experimental tools are necessary in order to quantify the domain patterns in ferroelectrics. This study on $BaTiO_3$ single crystals exemplifies how vector piezoresponse force microscopy can be used to obtain statistical information about domain directions. © *2010 American Institute of Physics*. [doi:10.1063/1.3467531]

I. INTRODUCTION

The behavior of a ferroelectric material under electrical or mechanical loading is a result of changes in its domain structure. Therefore, understanding their macroscopic properties demands knowledge about these changes.

The commercial interest in ferroelectric material for a wide range of applications, e.g., actuators, sensors, ferroelectric random access memory, etc., has led to high research interest in methods and models that can help to understand and optimize the application of this class of materials.

Nowadays models of ferroelectric materials can predict the qualitative features of ferroelectric switching, including hysteresis and butterfly loops.[1] One effective microelectromechanical model, first presented by Huber *et al.*,[2] simulates the response of polycrystals through incremental switching due to domain wall motion.[1] Following Pathak and McMeeking[1] one of the reasons why such models are beyond the state of the art is that actual domain patterns in a single grain within a polycrystal have been identified in only one or two special cases in $BaTiO_3$.[3]

The most suitable method that is able to deliver reliable data to optimize such models is the piezoresponse force microscopy (PFM). It offers the possibility to record the domain structure with high resolution and without the need of extensive sample preparation. It also allows changing the domain structure *in situ* by application of an electric field. Some studies have demonstrated that PFM can be used to reconstruct the domain structure.[4–6] However, PFM is also affected by a range of external influences that can alter the recorded data (more on that in Sec. II). In general, PFM measurements can deliver a lot of interesting information, which needs to be continually questioned to avoid misinterpretations.[7]

In 2006 Kalinin *et al.*[8] described an approach, called vector PFM (Vector PFM), for the characterization of the orientation dependence of electromechanical properties. In their work they discussed some approaches for PFM signal acquisition and calibration. However, the implementation of Vector PFM is not straight forward and the data presented, $PbTiO_3$ thin film and $LaBGeO_3$ crystallite, have complex domain structures that do not allow for a verification of the results. An attempt to use Vector PFM by McGilly *et al.*[7] in $BaTiO_3$ led to inconsistencies with the known crystallography of the samples.

In this work we propose to use a form of Vector PFM to map and quantify the local orientation of the polarization vectors. We chose a simple and well known $BaTiO_3$ structure to validate the approach. We aim to provide a tool that can be used to quantify changes in the domain structures of more complex systems such as lead zirconate titanates (PZT) and potassium sodium niobates (KNN) before and after poling experiments.

II. PFM

PFM is a contact imaging mode of the scanning probe microscope. In PFM a modulated voltage $V(\omega) = V_{ac}\cos(\omega t)$ of frequency ω and amplitude V_{ac}, is applied to a conductive probe that is in contact with the ferroelectric material. The electric field excites an oscillatory deformation of the surface, which are transferred to the cantilever. The cantilever movements are detected by a four quadrant photodetector, which can detect deflection and torsion movements. The signals are demodulated by Lock-in amplifiers and recorded with the atomic force microscopy system.

Deflection signals of the cantilever are related to normal surface displacements denoted vertical PFM (VPFM). Torsion signals are related to a tilt around the longitudinal cantilever axis, denoted lateral PFM (LPFM). To get full information of the surface displacements a second torsion signal is needed and measured by rotating the sample by 90°. The first LPFM signal is defined as Y signal and therefore denoted Y-LPFM, after rotation by 90° we define the signal as X-LPFM.

a)Electronic mail: g.schneider@tuhh.de.

 © 2010 American Institute of Physics

Downloaded 27 Aug 2010 to 134.28.92.9. Redistribution subject to AIP license or copyright; see http://jap.aip.org/about/rights_and_permissions

As mentioned before PFM is prone to artifacts that can strongly affect the collected data. Careful system calibration and correction of the recorded data are required for a reliable interpretation.

The first important contribution is a frequency dependent response reported by Jungk *et al.*[9] that analyzed this problem in great detail and proposed a practical method to minimize the error due to this frequency dependent response.

In PFM the sensitivity for lateral and vertical displacements of the tip are not the same.[10] However, in order to determine the domain directions the signals must be comparable. Kalinin *et al.*[8] proposed a method for correcting the intensities using the ratio between VPFM and LPFM measured in a known *a-c* domain structure (for example, in $BaTiO_3$).

Another contribution to the PFM signals comes from the buckling of the cantilever; which originates from in-plain domains oriented parallel to the cantilever axis and will give a signal that is indistinguishable from the VPFM signal.[11,12] Recently, Johann *et al.*[13] analyzed $LiNbO_3$ nanoparticles and were able to clearly separate deflection from buckling in the VPFM signal by controlled rotation of the sample.

Finally, it must be noted that it is imperative that exactly the same region is analyzed; in each measurement both LPFM and VPFM can be recorded simultaneously. But to measure the orthogonal LPFM signal, a second measurement is needed with the sample rotated by 90°.

III. METHOD

Measurements were performed on the (001) crystal plane of a $BaTiO_3$ single crystal. The orientation of the crystal was confirmed with x-ray diffraction. The sample was polished with diamond suspension down to 0.25 μm and the final step was done with an etching agent (Mastermet, Bühler AG Düsseldorf, Germany).

The PFM measurements were made with a Pt/Ir conductive tip (Nanosensors, Neuchatel, Switzerland) at $\omega = 10$ kHz and $V_{ac} = 20$ V_{PP} applied to the tip. The PFM signals were demodulated with two Lock-in amplifiers (Signal Recovery 7225 and 7265, AMETEK, Wokingham, United Kingdom).

As mentioned before, to acquire two orthogonal LPFM signals two measurements are needed. It is mandatory for the analysis that both measurements are exactly at the same place; otherwise artifacts can be created in the images due to wrong superposition of the three images. Measuring exactly at the same place is a difficult task and sometimes may require extra measurements to locate the exact area again; which especially in polycrystalline samples can lead to tip wear which influences the PFM signal. To ensure a correct superposition of the scans (X-LPFM, Y-LPFM, and VPFM) we implemented a technique called "template matching."

In the "template matching"[14] method a part of one image is used as a template which is searched in the other image. The convolution will be the highest at the place where the template matches the image, in this case large image values are multiplied by large template values. In our case part of the topography image before rotation is used as a template which is compared with the topography image recorded after the rotation. The template can also be rotated to compensate for deviations in the rotation angle during the measurement. Once the maximum is found, and consequently the best matching of the template and the image, the pixel coordinates are recorded and only the overlapping areas of the images are left. Any small deviation on the rotation angle (that is set to 90°) is also recorded.

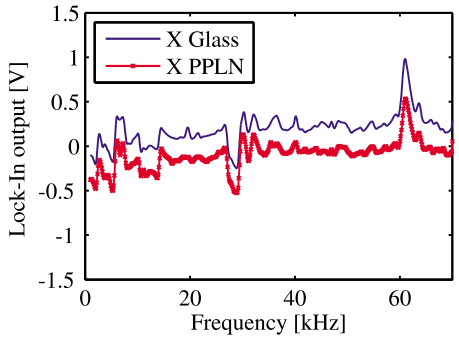

FIG. 1. (Color online) VPFM-frequency spectra for-Z face of a PPLN and glass. As the signal recorded glass cannot originate from a piezoelectric effect it is attributed to a system inherent background which also shows up in PPLN. X is the in-phase component of the Lock-in amplifier.

Before a detailed PFM analysis is possible an offset correction due to the nonuniform frequency response of the system is necessary. The frequency response measured on glass and $LiNbO_3$ with our equipment shows the same behavior as that reported by Jungk *et al.*[9] Figure 1 shows the VPFM frequency spectra measured on glass and in a-Z face of a periodically poled $LiNbO_3$ (PPLN). The curves denote the Lock-in amplifier X output for each sample. The determination of the offset was done using a glass slide and with the tip at rest (not scanning) immediately after the measurements in the ferroelectric sample, using exactly the same configuration (cantilever, laser position on the cantilever, ω and V_{ac}). It can be seen that glass, being nonpiezoelectric, shows a signal under the PFM operating conditions. This is due to the mechanics and electronics of the system and must be eliminated for a proper PFM analysis.

The difference between the $BaTiO_3$ and glass PFM signals is therefore taken as the corrected PFM signal, Eq. (1) is then applied to correct the VPFM signal

$$P_z^{\text{corrected}}(\omega) = V_{\text{Lock-in}}^{\text{VPFM}}(\omega, \text{BaTiO}_3) - V_{\text{Lock-in}}^{\text{VPFM}}(\omega, \text{glass}). \tag{1}$$

For the LPFM signals it turned out that the offset is much smaller than the signal measured in the sample, so that

$$V_{\text{Lock-in}}^{\text{LPFM}}(\omega, \text{glass}) \approx 0. \tag{2}$$

Hence we assumed

$$P_{x,y}^{\text{corrected}} = P_{x,y}^{\text{measured}}. \tag{3}$$

To correct the different displacements of the tip (for deflection and torsion) we choose the approach suggested by Kalinin *et al.*[8] Taking a $BaTiO_3$ (0 0 1) plane, for example, the LPFM signal is only present in *a*-domains while VPFM signal is only present in *c*-domains. Therefore, one can determine the correction factor of LPFM and VPFM by com-

Downloaded 27 Aug 2010 to 134.28.92.9. Redistribution subject to AIP license or copyright; see http://jap.aip.org/about/rights_and_permissions

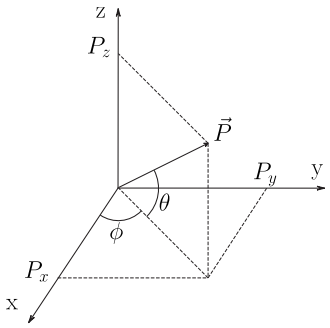

FIG. 2. Scheme showing the spherical coordinate system.

paring the signal from both different regions. In practice, we use the average signal from the *c*-domain (VPFM) area compared with the average signal from the *a*-domain (LPFM) area to find the correction factor α, as denoted in Eq. (4)

$$\alpha = \frac{\frac{\Sigma_1^m |\mathrm{LPFM}|}{m}}{\frac{\Sigma_1^n |\mathrm{VPFM}|}{n}}, \tag{4}$$

where m and n denotes the summation over all LPFM pixels and VPFM pixels, respectively. The α factor measured in the *a*-*c* domain structure is equal to 3.78 ± 0.1.

It is known that in $BaTiO_3$ the magnitude of the polarization vector $\vec{P}$ in *a* and *c*-domains is the same. Thus the signal was corrected so that the maximum VPFM signal is equal to the maximum LPFM signal, as follows:

$$P_z = \alpha P_z^{\mathrm{corrected}}, \tag{5}$$

$$P_{x,y} = P_{x,y}^{\mathrm{measured}}. \tag{6}$$

The correct signals (P_x, P_y, P_z) are then transformed into spherical coordinates (θ, ϕ, P) with Eqs. (7)–(9),

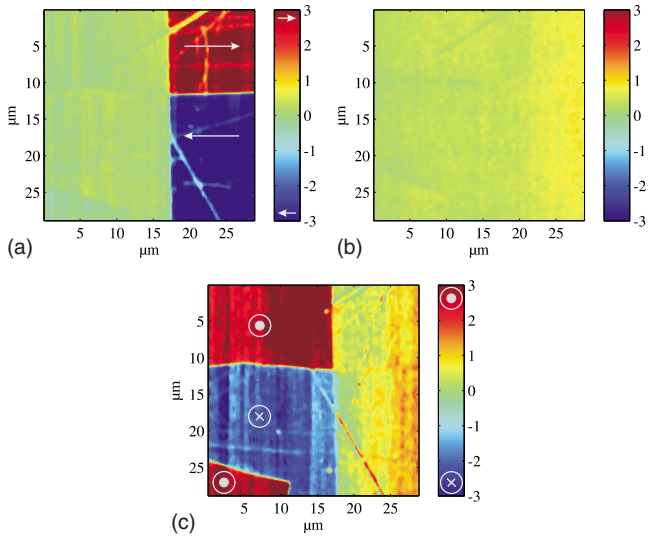

FIG. 3. (Color online) (a) P_x, (b) P_y, and (c) P_z signals as depicted in Eqs. (5) and (6). The values are given in units of volts (V). Note that scratches on the surface are clearly visible in the PFM images.

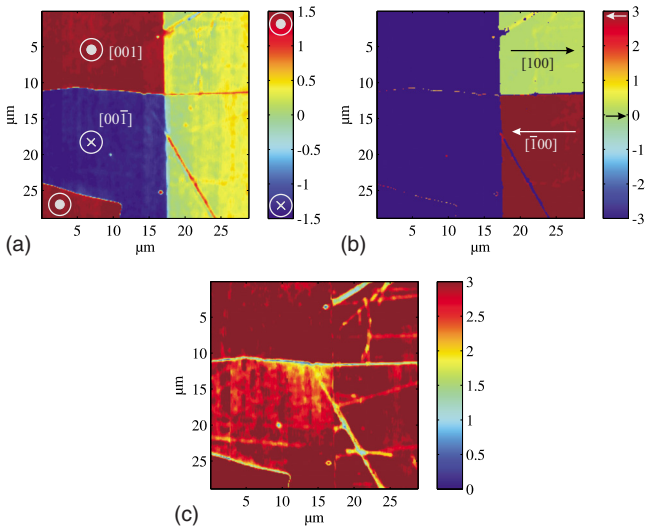

FIG. 4. (Color online) PFM-images of Fig. 3 transformed to spherical coordinates. The θ and ϕ images (in radians) are in full agreement with the domain structures shown by the symbols. The *P*-image indicates whether the magnitude of the *P*-vector (in volts) is constant.

$$\theta = \arcsin\left(\frac{P_z}{P}\right), \tag{7}$$

$$\phi = \arctan\left(\frac{P_y}{P_x}\right), \tag{8}$$

$$P = |\vec{P}| = \sqrt{P_x^2 + P_y^2 + P_z^2}, \tag{9}$$

where θ is the zenith (elevation) angle measured in radians from the x-y plane, ϕ is the azimuthal angle in radians, and *P* is the magnitude in volts. Figure 2 shows the spherical coordinate system.

For each image, the values of θ, ϕ, and *P* are plotted in a histogram summing the number of occurrences (pixels) of each value.

IV. RESULTS AND DISCUSSION

The $P_{x,y,z}$ values as given by Eqs. (5) and (6) of an 30×30 μm^2 area on the $BaTiO_3$ crystal are shown in Fig. 3. Note that scratches in the surface are clearly visible on the PFM images.

Because the crystallographic plane of the imaged surface is known to be (1 0 0), we correlated the orientation information from PFM images with the crystallographic directions. In a tetragonal crystal system there are only six possible orientations along the axes of the coordinate system. In our case a positive P_z value indicates a polarization in the [0 0 1] direction while a negative P_z value indicates the

TABLE I. Quantification of the domain orientations for the $BaTiO_3$ sample.

	$BaTiO_3$ sample			
Direction	[0 0 1]	[0 0 $\bar{1}$]	[1 0 0]	[$\bar{1}$ 0 0]
% of the image	27.5	32.4	15	25.1

Downloaded 27 Aug 2010 to 134.28.92.9. Redistribution subject to AIP license or copyright; see http://jap.aip.org/about/rights_and_permissions

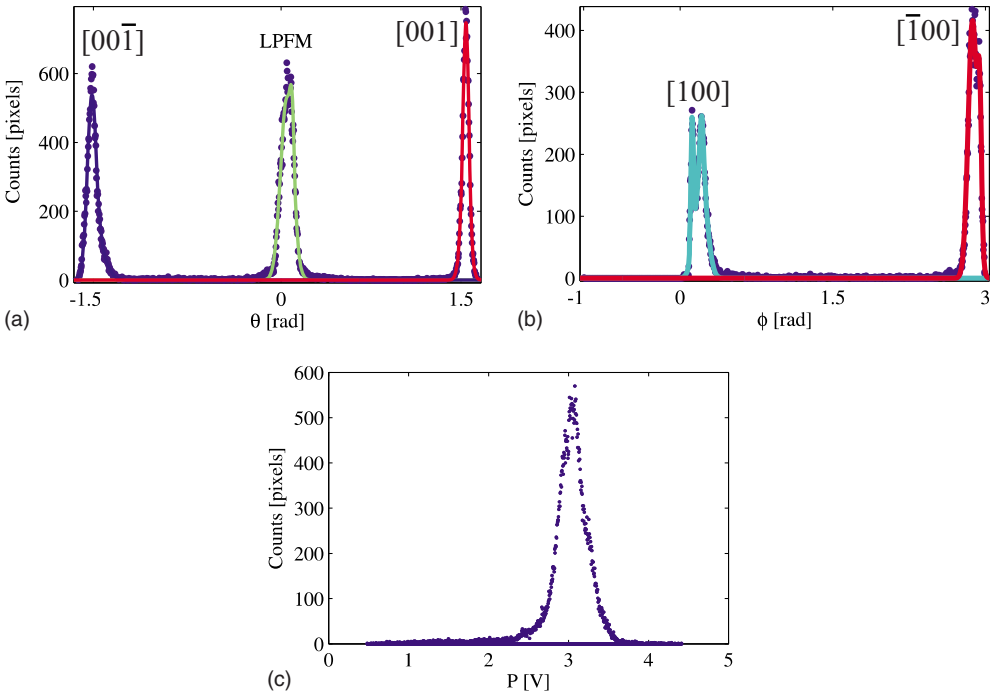

FIG. 5. (Color online) Histograms and corresponding directions of the polarization vectors.

[0 0 $\bar{1}$] polarization direction and so on. In the same way we can attach specific angles in θ or ϕ to a corresponding polarization direction.

After the conversion into spherical coordinates the data is plotted as θ, ϕ, and P images (Fig. 4). In the θ image [Fig. 4(a)] domains in the [0 0 $\bar{1}$] and [0 0 1] polarization directions can be identified. The ϕ image [Fig. 4(b)] allow us to identify domains in the [1 0 0] and [$\bar{1}$ 0 0] polarization directions. The left side of the ϕ image denotes a region where the angle ϕ is not defined because θ is normal to the surface.

To quantify the information on the θ, ϕ, and P images we plot histograms from each image. The histograms show the number of occurrences (pixels) for the given value. Each histogram is fitted with an appropriate function; summing the total counts for each peak and dividing by the total number of counts from the image we are able to quantify the area fraction of domains in that specific direction (see Table I).

The histogram for the θ image [Fig. 5(a)] shows peaks at approximately 0 and ± 1.5 rad and can be related to the polarization directions as indicated. The peak at 0 rad accounts for the sum of LPFM signals.

The histogram for the ϕ image [Fig. 5(b)] show peaks at approximately 0.1 rad and 2.9 rad, which represent [1 0 0] and [$\bar{1}$ 0 0] directions, respectively.

The histogram for the P image [Fig. 5(c)] shows a narrow distribution of the signal (magnitude) with mean of 3.0 ± 0.5 V.

In the ideal case, for the given sample, the expected values are: for θ peaks 0 and $\pm \pi/2$ and for ϕ peaks at 0 and π. Our result is close to this theoretical result and shows the practical limits but also the possibilities of the procedure.

The results of the quantification of the histograms data is given in Table I.

A. Vector representation

To this point we have shown how to quantify domains in different directions. It is natural to represent this direction by vectors in space. That has the advantage of an easy domain wall identification.

To demonstrate this representation we first clustered the domain data using the vector angles for each pixel. The angle for each domain region is then averaged to a representative value and plotted in an image (Fig. 6) that represents the clusters with different colors(regions 1, 2, 3, and 4 in Fig. 6). The same representative values are used to plot three-dimensional (3D) vectors in Fig. 7 using the same colors as the cluster image (regions 1, 2, 3, and 4), the magnitude of each vector is weighted by the size of the cluster.

The vector representation of the domain directions allows for the identification of the domain wall types, for ex-

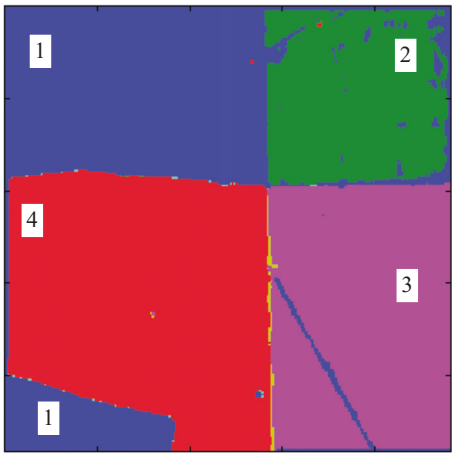

FIG. 6. (Color online) Image showing the clusters calculated from the domain structure. Scratches and imperfections in the clustering procedure are also visible.

Downloaded 27 Aug 2010 to 134.28.92.9. Redistribution subject to AIP license or copyright; see http://jap.aip.org/about/rights_and_permissions

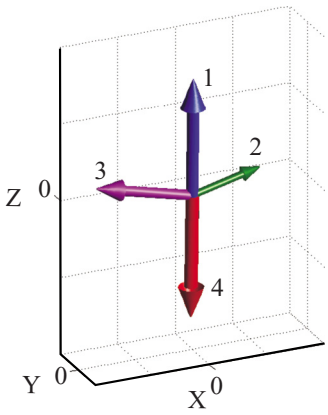

FIG. 7. (Color online) 3D vector representation of the clusters shown in Fig. 6 each vector color corresponds to the same color in the cluster image (Fig. 6). This representation allows for an easy interpretation of the domain directions and domain walls.

ample, 90° domain walls between the blue and violet vectors (1 and 3) and 180° domain walls between the red and blue vectors (1 and 4). Such analysis is simple in our $BaTiO_3$ single crystal example but rather complex in polycrystals such as PZT or sodium niobates (KNN).

V. SUMMARY AND CONCLUSIONS

In this work we demonstrated the ability of Vector PFM to quantify the distribution of domain directions in a $BaTiO_3$ single crystal.

The "template match" technique improves the precision of matching the measured PFM signals, locating the three different signals in the same x-y coordinates in the images, with good topography references the technique provides an exact match. Correcting and transforming the corrected signals, Y-LPFM, X-LPFM, and VPFM, into spherical coordinates provides a way to quantify the domains orientation. Even without the knowledge of the crystallographic orientation of the crystal surface one can still quantify the relative orientation of the domains.

The representation using 3D vectors allows for an easier determination of the domain wall directions. The example given for the $BaTiO_3$ single crystal demonstrates the applicability of the method which, considering the careful calibration of the signals, can be applied in polycrystals that have a much more complex domain structure.

[1]A. Pathak and R. M. McMeeking, J. Mech. Phys. Solids **56**, 663 (2008).
[2]J. E. Huber, N. a. Fleck, C. M. Landis, and R. M. McMeeking, J. Mech. Phys. Solids **47**, 1663 (1999).
[3]G. Arlt, J. Mater. Sci. **25**, 2655 (1990).
[4]A. Roelofs, U. Böttger, R. Waser, F. Schlaphof, S. Trogisch, and L. M. Eng, Appl. Phys. Lett. **77**, 3444 (2000).
[5]L. M. Eng, H.-J. Güntherodt, G. A. Schneider, U. Köpke, and J. Munoz Saldana, Appl. Phys. Lett. **74**, 233 (1999).
[6]R.-P. Herber, G. A. Schneider, S. Wagner, and M. J. Hoffmann, Appl. Phys. Lett. **90**, 252905 (2007).
[7]L. McGilly, D. Byrne, C. Harnagea, A. Schilling, and J. Gregg, J. Mater. Sci. **44**, 5197 (2009).
[8]S. V. Kalinin, B. J. Rodriguez, S. Jesse, J. Shin, A. P. Baddorf, P. Gupta, H. Jain, D. B. Williams, and A. Gruverman, Microsc. Microanal. **12**, 206 (2006).
[9]T. Jungk, A. Hoffmann, and E. Soergel, Appl. Phys. Lett. **91**, 253511 (2007).
[10]F. Peter, A. Rudiger, R. Waser, K. Szot, and B. Reichenberg, Rev. Sci. Instrum. **76**, 046101 (2005).
[11]B. D. Huey, C. Ramanujan, M. Bobji, J. Blendell, G. White, R. Szoszkiewicz, and A. Kulik, J. Electroceram. **13**, 287 (2004).
[12]T. Jungk, A. Hoffmann, and E. Soergel, New J. Phys. **11**, 033029 (2009).
[13]F. Johann, T. Jungk, S. Lisinski, A. Hoffmann, L. Ratke, and E. Soergel, Appl. Phys. Lett. **95**, 202901 (2009).
[14]R. Brunelli, *Template Matching Techniques in Computer Vision: Theory and Practice* (Wiley, Chichester, 2009).

Downloaded 27 Aug 2010 to 134.28.92.9. Redistribution subject to AIP license or copyright; see http://jap.aip.org/about/rights_and_permissions